Geochemistry, Geophysics, Geosystems

RESEARCH ARTICLE
10.1029/2020GC008976

Residuals to the CHAOS-6 Geomagnetic Field Model Caused by Magnetospheric Currents During Enhanced Magnetic Activity

Hermann Lühr[1] **and Yun-Liang Zhou**[2]

[1]GFZ, German Research Centre for Geosciences, Section 2.3, Geomagnetism, Potsdam, Germany, [2]Department of Space Physics, School of Electronic Information, Wuhan University, Wuhan, China

Key Points:

- The geomagnetic field model CHAOS-6 represents insufficiently the ring current effect during times of enhanced magnetic activity
- The residuals, observations minus model, show local time dependences and seasonal dependences in the two hemispheres
- The residuals show a systematic variation with longitude; this can be interpreted as a Universal Time dependence

Correspondence to:
H. Lühr,
hluehr@gfz-potsdam.de

Citation:
Lühr, H., & Zhou, Y.-L. (2020). Residuals to the CHAOS-6 geomagnetic field model caused by magnetospheric currents during enhanced magnetic activity. *Geochemistry, Geophysics, Geosystems*, *21*, e2020GC008976. https://doi.org/10.1029/2020GC008976

Received 11 FEB 2020
Accepted 22 APR 2020
Accepted article online 25 APR 2020

Abstract Thanks to mapping missions, like Ørsted, CHAMP, and Swarm, we have gained a detailed understanding of the geomagnetic field. High-resolution models like POMME, GRIMM, or CHAOS are able to describe the main parts of the Earth's magnetic field reliably. These models represent well contributions from the core and crustal fields. But their validity of describing magnetospheric field effects is limited to low activity periods (Kp ~ 0–2). Here, we study the differences between CHAMP magnetic observations and the predictions from CHAOS-6-x9, a recent version, outside this validity range. Systematic residuals appear at times of elevated activity. Mean amplitudes at the equator grow up to 12 nT around 20 hr magnetic local time for magnetic activity around Kp = 4.7. Negative residuals are obtained in the evening to midnight sector and positive ones in the morning. A seasonal dependence of the magnetospheric currents causes more negative deflections of the residuals in the winter than in the summer hemisphere. This hemispheric asymmetry cannot be accounted for by a degree 1 spherical harmonics function. A surprising observation is that the residuals show a clear longitude dependent pattern, which changes with local time. The analysis reveals that this feature can be interpreted as a Universal Time dependence of the residuals with a peak-to-peak amplitude of about 8 nT and a period of 12 hr at an activity level of Kp = 4.7. All these results call for a better parameterization of the magnetospheric current effects in a geomagnetic field model that is reliable at least up to moderate activity levels.

1. Introduction

The Earth's magnetic field, as we observe it on ground or at low-Earth orbit, is representing the sum of contributions from many different sources. The largest part, more than 90%, originates from the geodynamo in the outer, liquid core of the Earth. Another part results from the magnetization of the sediments and rocks. Furthermore, electric currents in the upper atmosphere and near-Earth space can, in particular during times of enhanced magnetic activity, contribute a significant fraction to the geomagnetic field. One aim of recent magnetic field research is to separate the various parts, in order to study their characteristics and temporal evolution in more details. Important steps in that direction are the developments of high-resolution geomagnetic field models. Prime bases for such enterprises are the data from dedicated magnetic field mapping missions such as Ørsted, CHAMP, and Swarm, covering the past 20 years. And in addition, the measurements of the nearly 150 magnetic observatories are a great help in this effort. Meanwhile, several model families have evolved from these activities. They include POMME (e.g., Maus et al., 2010), GRIMM (e.g., Lesur et al., 2008, 2015), CHAOS (e.g., Finlay et al., 2016; Olsen et al., 2014), and the comprehensive model CM (e.g., Sabaka et al., 2002, 2018). Commonly, these models characterize the dominating core field, the crustal field, and the magnetic fields from large-scale magnetospheric currents. Just the CM model is also estimating the effects of ionospheric currents. With the accumulation of well distributed high-resolution satellite measurements over two decades, these models have become very reliable. Due to the unpredictable evolution of the Earth's magnetic field, the model parameters need regular overhauls, typically once a year, to extend their validity to actual dates.

An important application of these geomagnetic field models is to remove the large contributions from the prime sources to the observed geomagnetic field values when studying weaker effects such as ionospheric currents, plasma irregularities, or even ocean tidal motions. Largest uncertainties are introduced into the field models by the magnetospheric currents. It has so far not been possible to characterize their

distribution and variability properly, especially during times of elevated magnetic activity. For mitigating that problem, most of the above listed model families select only data from quiet periods, for example, Kp = 0–2. This approach of data selection is justified for representing internal field sources, such as core field, crustal field, or ocean current signals most accurately. Also CHAOS-6 is a quiet-time magnetic field model and is therefore not expected to perform so well during more active times. However, for certain studies, such as ionospheric currents, it would be desirable to have a geomagnetic field model that accounts reliably for large-scale magnetospheric current effects up to moderate activity levels, for example, Kp < 4.

For our model/observation comparison, we have chosen CHAOS-6 (Finlay et al., 2016). This family is frequently used in magnetic field studies, and the considered version is the most recent. The magnetic fields from magnetospheric currents are represented by external spherical harmonic functions. Olsen et al. (2014) give in their Section 3 a detailed description of the external field parameterization in the CHAOS model. For the convenience of the reader, the important parts of the description are repeated here:

$$V^{ext}=a\sum_{n=1}^{2}\sum_{m=0}^{n}\left(q_n^m\cos mT_d+s_n^m\sin mT_d\right)\left(\frac{r}{a}\right)^n P_n^m(\cos\theta_d)+a\sum_{n=1}^{2}q_n^{0,GSM}R_n^0(r,\theta,\varphi), \quad (1)$$

where a = 6,371.2 km is the radius of the Earth, r is the radial distance of measurement and P_n^m represents the Schmidt seminormalized Legendre functions; θ_d and T_d are dipole colatitude and dipole local time, respectively. The degree-1 coefficients in Solar-Magnetic (SM) coordinates depend explicitly on time and are further expanded as

$$q_1^0(t)=q'^0_1\left[RCe+RCi\left(\frac{a}{r}\right)^3\right]+\Delta q_1^0(t), \quad (2a)$$

$$q_1^1(t)=q'^1_1\left[RCe+RCi\left(\frac{a}{r}\right)^3\right]+\Delta q_1^1(t), \quad (2b)$$

$$s_1^1(t)=s'^1_1\left[RCe+RCi\left(\frac{a}{r}\right)^3\right]+\Delta s_1^1(t), \quad (2c)$$

where the term in brackets describes the magnetic field contribution due to the magnetospheric ring current and its Earth-induced counterpart, as given by the RC index, which is similar to D_{ST}, $RC(t) = RCe(t) + RCi(t)$, respectively (see Olsen et al. (2014), Section 2.2). If RC provides a perfect description of the magnetospheric field at satellite altitude, the values of the regression coefficients would be $q'^0_1 = -1$, $q'^1_1 = s'^1_1 = 0$ and with vanishing "RC baseline corrections" $\Delta q_1^0(t)$, $\Delta q_1^1(t)$, and $\Delta s_1^1(t)$. We allow for deviations from these values and coestimate the regression factors q'^0_1, q'^1_1, s'^1_1 and solve for the baseline corrections in bins of 5 days (for $\Delta q_1^0(t)$) and 30 days (for $\Delta q_1^1(t)$, $\Delta s_1^1(t)$), respectively. The q_2^m, s_2^m , and the two coefficients in Geomagnetic-Solar-Magnetospheric (GSM) coordinates, $q_n^{0,GSM}$, are considered to be static. R_n^0 are modified Legendre functions accounting for induced field contributions due to the wobble of the GSM z-axis with respect to the Earth's rotation axis. Definitions of the SM and GSM coordinate systems can be found in Hapgood (1992).

The aim of this study is to find out how well does the used field description represent the actual magnetospheric currents, outside the validity range of the model. For addressing this question, we make use of the CHAMP magnetic field measurements. We will check the quality of the CHAOS-6 model predictions for different levels of magnetic activity. Particularly useful for this purpose are the CHAMP data from the first half of the mission. During that period, the activity varied from its peak to low levels.

In the sections to follow, we will first introduce the data set used in this study. Section 3 presents derived differences between observation and model and shows how they depend on magnetic activity, local time, season, and longitude. The Discussion in section 4 tries to interpret the causes that are responsible for the derived residuals. Section 5 finally summarizes the important results and makes suggestions for an improved modeling of the large-scale magnetospheric currents.

2. Data Set

For the study presented here, we make use of the high-resolution CHAMP magnetic field data. The CHAMP satellite was launched into a circular near-polar orbit (inclination: 87.3°) with an initial altitude of 456 km on 15 July 2000 (Reigber et al., 2002). By the end of the mission, 19 September 2010, the orbit had decayed to 250 km. The Fluxgate Magnetometer (FGM) on board CHAMP recorded the vector magnetic field every 0.02 s with a resolution of 0.1 nT. The FGM magnetic field readings are calibrated routinely by using the observations of the onboard absolute scalar Overhauser Magnetometer. In this study, the fully calibrated Level-3 magnetic field products (product identifier: CH-ME-3-MAG) are used (Rother & Michaelis, 2019). Magnetic field vectors are provided in the North-East-Center (NEC) frame with a time resolution of 1 Hz. We employ in this study data of the 5 years from 2001 to 2005, which experienced solar and magnetic activities from high to moderate levels. There is no other 5-year period during the magnetic satellite era with a comparable spread of activity. The satellite orbital plane covers all local times within 130 days when considering both upleg and downleg arcs. Five years of CHAMP magnetic field observations are just needed to sample all local times 14 times, evenly distributed over all seasons.

For comparison, we have chosen the CHAOS model. This is presently frequently used in studies of minor magnetic field contributors such as ionospheric currents, plasma irregularities, or even ocean tides. CHAOS provides one of the best representations of the major geomagnetic field contributors. Model predictions of the field have been calculated for every time and position of the CHAMP Level 3 data over the considered 5 years. For this comparison, the full capability of the CHAOS model was utilized, including the contributions of the core field, crustal field and magnetospheric currents (see Finlay et al., 2016).

3. Model to Observation Comparisons

Of particular interest, here are the residuals between magnetic field observations and the predictions of the recent version, the CHAOS-6-x9 model. We are not interested in randomly distributed deviations but rather want to find out systematic differences between the two datasets. For that reason, we take a statistical approach for determining the dependences of residuals on various parameters such as magnetic activity, season, local time, and position. It is well known that largest uncertainties result from deficits in properly modeling the magnetospheric currents. Therefore, we focus our attention to residual effects of the magnetospheric ring current. CHAOS is not estimating field from ionospheric currents, for that reason, only differences from the nightside are considered in this study, when these currents are weak.

Figure 1 presents for two examples latitude profiles of differences between magnetic field observations and concomitant CHAOS-6 model predictions. Shown are the total field residuals shortly before midnight for a quiet day (left, Kp = 0.7) and for a moderately disturbed day (right, Kp = 3.3). Here and in the rest of the paper, we make use of total field residuals because they are less noisy and less affected by ionospheric F-region currents, thus better representing magnetospheric contributions. During the quiet day only, small residuals of the order of ±1 nT are observed at low and middle latitudes. These can be related to weak ionospheric F-region currents at night. Conversely on the more active day, the residuals exceed peak-to-peak amplitudes of 10 nT. The rather symmetric depletion of the total field component with a minimum near the magnetic equator and zero-crossings just above ±30° magnetic latitude (MLat) are typical signatures of residual ring current fields. Already this example shows that CHAOS-6 has deficits in representing the magnetospheric fields properly for moderately enhanced activity conditions.

As mentioned in section 1, the CHAOS-6 model construction is based on data from quiet periods (Kp = 0–2). It is therefore expected that it cannot well represent magnetospheric currents during active times. In the subsequent sections, we present the mean characteristics of the residuals in total field for different levels of magnetic activity and try to interpret them in terms of ring current features.

3.1. Magnetic Activity Dependence of Residuals

The 5 years considered for our analysis range from the peak of solar cycle 23 down to the moderate solar flux levels with a mean value of the radio flux index F10.7 = 137.4 sfu. This period also includes the strongest magnetic storms during that cycle. This wide variety of events allows for studying various details of the residuals.

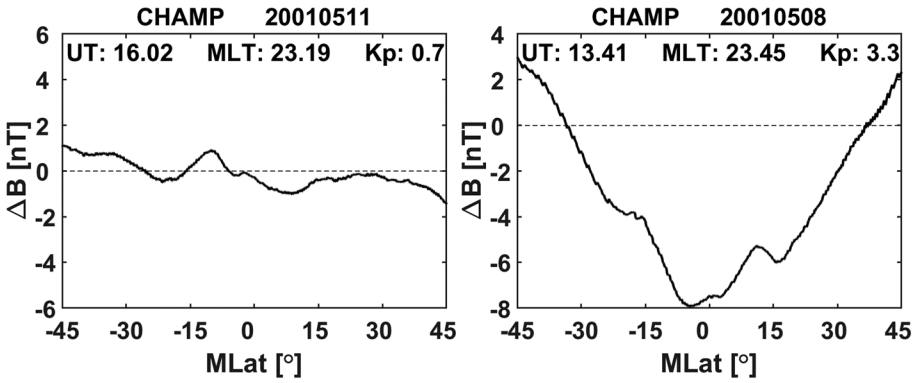

FIGURE 1. Two examples of total magnetic field residuals (observations minus CHAOS-6 predictions) versus dipole magnetic latitude (MLat) for a quiet day (left) and a moderately disturbed (right). In both cases, examples have been taken from magnetic local times (MLT) shortly before midnight.

Figure 2 shows for low and mid-latitude profiles of obtained average total field residuals (observations minus model values) for three activity ranges (Kp = 0 to 1, 2 to 3, and 4–9) and three local times (MLT = 19, 24, and 05). These multiyear averages are smoothing out any annual variations of the latitude profiles. Here, we used magnetic dipole latitude (MLat) and dipole magnetic local time (MLT). For the coordinate transformation, we have chosen a position of the northern geomagnetic dipole at 79.75°N and 71.81°W according to the coefficients of the DGRF-2005 model.

For low activity (Kp=0 to 1), only small mean residuals result, of order 1 nT. They can be attributed to nighttime currents in the ionospheric F-region. The small hump at the equator around 05 MLT has been identified as an early signature of the equatorial electrojet. Under these quiet conditions, CHAOS-6 is very efficient to remove on average the three considered contributions from core, crust, and magnetosphere fields. However, when leaving the validity range of the model, already for moderate magnetic activity (Kp=2 to 3), the situation starts to change. Significant negative residuals appear in the evening hours and positive during early morning. This trend is even more pronounced for Kp>4 conditions (mean value Kp~4.7). Similar kinds of residuals have been reported by Stolle et al. (2016). It is well known that the magnetospheric ring current causes negative deflections of the total field at low latitudes. Our residuals indicate that the CHAOS-6 model underestimates the ring current signal in the evening and overestimates it during morning hours. The transition between the two cases occurs some hours after midnight. In the following parts, we focus on the residuals from periods of enhanced magnetic activity.

In order to obtain more quantitative results, we have tried to estimate the remaining ring current effect, ΔRC. We assume a homogeneous external degree 1 field that adds to the Earth's dipole field. In that case, the resulting total field, ΔB residuals can be expressed as

$$\Delta B = -\Delta RC \frac{3sin^2(ß) - 1}{\sqrt{1 + 3sin^2(ß)}}, \quad (3)$$

where $ß$ is the dipole latitude. Values of ΔRC are determined by fitting Equation 3 to the observed ΔB profiles. At a latitude, $ß = 35.26°$ ($0 = 3\ sin^2(ß)\ -1$), the ring current effect is expected to vanish. Therefore, we limit our fitting to the latitude range of ±33° MLat. Residual ring current effects have been determined for four activity level separately for all the nighttime hours (18–06 MLT). Figure 3 shows, as examples, the estimated ΔRC values versus the mean a_P index for the 3 hr, 19, 24, 05 MLT. Since the mean activity differs between the local time hours, the resulting ΔRC values are connected by fitting a quadratic function. This is the lowest degree polynomial for connecting the points. Here, we confirm the earlier impression. During the first half of the night, CHAOS-6 underestimates the ring current effect; around early morning, it overestimates the effect. This trend gets larger towards higher magnetic activity.

A complete overview of the activity dependent variation of ΔRC with local time hours is given in Figure 4. For obtaining a smooth distribution, ΔRC values at the different levels of magnetic activity were derived from the quadratic equations, as shown in the frames of Figure 3. For connecting the results along the MLT axis, the values of neighboring hours were taken into account as $y_n = 0.25\ x_{n-1} + 0.5\ x_n + 0.25\ x_{n+1}$.

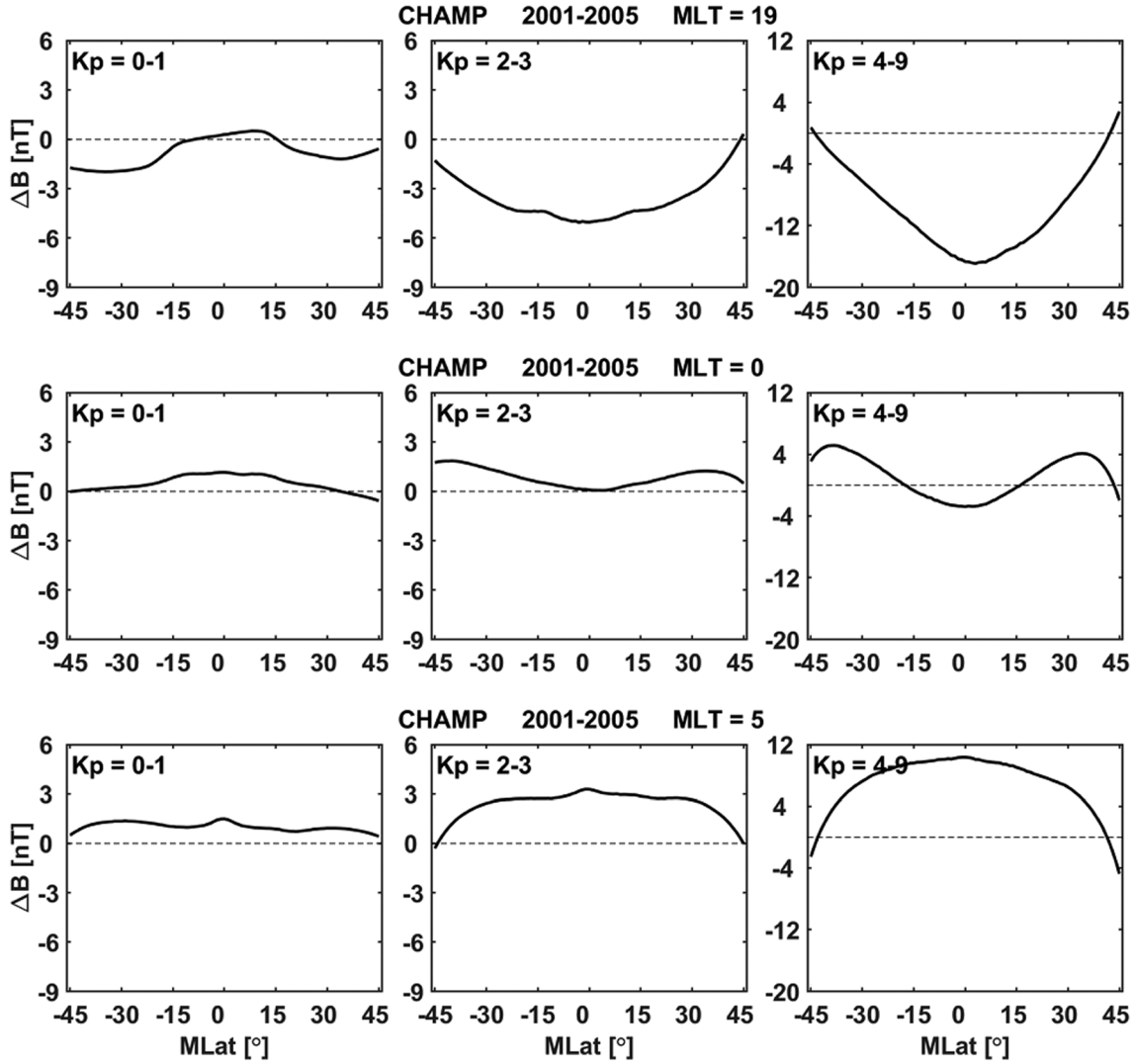

FIGURE 2. Latitude profiles of mean total field residuals for different levels of magnetic activity (increasing activity from left to right columns). Examples are presented for the local times 19, 24, and 05 MLT in the top, middle, and bottom rows, respectively. These profiles represent the 5-year averages. Note the different amplitude scale for high activity cases in the right column.

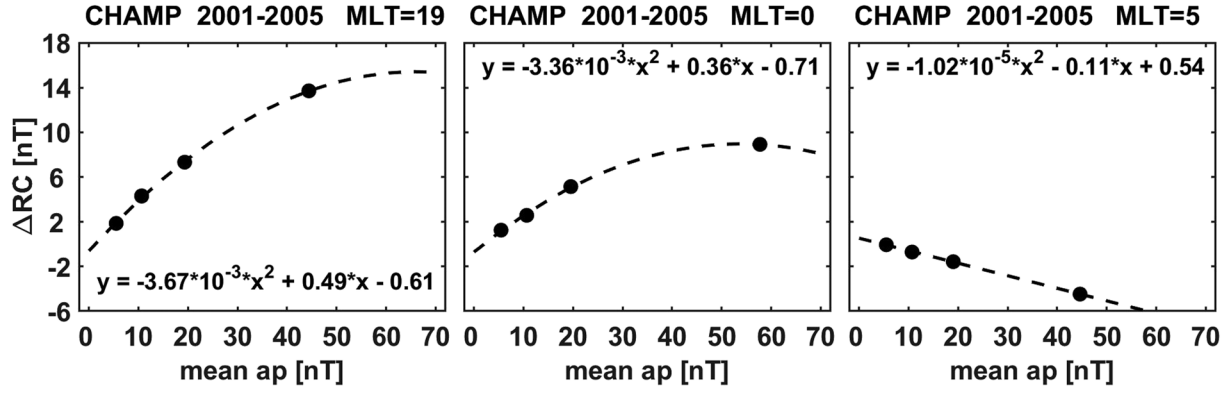

FIGURE 3. Estimated residual ring current index, ΔRC, as function of the magnetic activity index a_P. Examples are shown for the local times 19, 24, and 05 MLT.

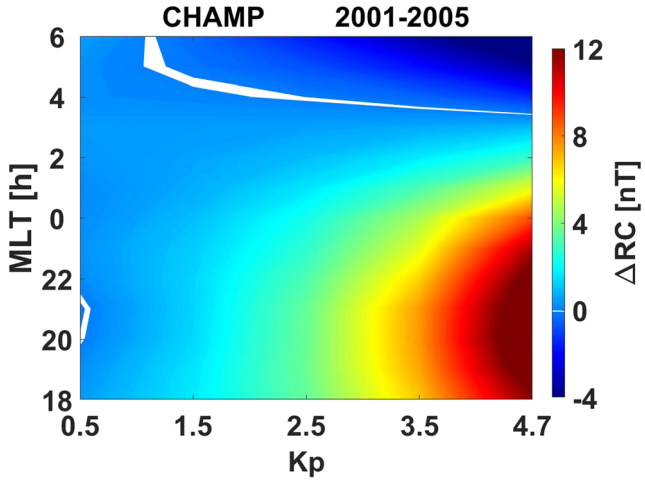

FIGURE 4. Distribution of mean ring current residuals, ΔRC, in a local time versus magnetic activity frame.

For quiet times (Kp = 0–1), very small to vanishing residuals are found, confirming the quality of the CHAOS-6 model. Deviations increase progressively towards higher Kp values. We could not go beyond Kp = 4.7 because of a lack of sufficient events at all the nighttime hours for obtaining reliable mean values. The largest underestimation of the ring current effect, reaching mean values of 12 nT, occurs around 20 MLT. And this trend of positive residuals during pre-midnight hours is in principle true, although with varying amplitudes, for all levels of activity. A switch in polarity occurs around 03 and 04 MLT, marked by the white bar. Here, the overestimations, negative residuals, reach only one-third the amplitudes of the underestimations. Also, these early morning deviations do not change their characteristics much with local time, just their amplitude with increasing activity.

3.2. Seasonal Dependence of Residuals

So far, we have looked at 5-year averages of the total field residuals. From earlier studies (e.g., Lühr & Zhou, 2020), it is known that the asymmetric ring current effect is more intense in the winter hemisphere than on the summer side. It may thus be expected that also the residuals from the model estimates show a seasonal effect. This is exactly what we observe. Figure 5 shows for three local time hours latitude profiles of total B residuals during magnetically active periods separately for the three Lloyd seasons. These seasons comprise for June solstice, the months May–August, for December, solstice the months November–February, and for the combined equinoxes, the remaining four months. In the upper left corner, the mean a_P index is listed of all the passes considered in a frame. As we know, the level of activity can explain most of the observed differences in amplitude.

For equinox conditions, quite symmetric latitude profiles result. They are well comparable with the multi-year averages for high activity in the right column of Figure 2. During solstice seasons, however, at all the local time hours, a clear hemispheric asymmetry emerges. Residuals are significantly more positive in the winter than in the summer hemisphere. Such a seasonal asymmetry of the magnetospheric current effects is obviously not well corrected by the CHAOS model.

3.3. Longitude Dependence of Residuals

It is commonly agreed that the asymmetric parts of the ring current effect vary with local time, in particular during active periods. Conversely, there has been little attention paid so far to a possible UT dependence of the current intensity. In this study, we check whether there are certain longitudinal patterns observable in the total field residuals. For that purpose, we make use of the residuals from our highest activity class (Kp > 4) because effects are expected to be clearest in those cases. Residual profiles of a local time hour are sorted into 45° wide longitude bins. For all, the eight longitude by 13 MLT bins mean ΔRC values are estimated according to Equation 3. Figure 6a shows the obtained distribution of deviations in a local time versus longitude plot. There is a clear longitude variation emerging. Peak ΔRC values reach even 18 nT, significantly larger than obtained from the longitudinal average in Figure 4.

A convenient way of characterizing systematic longitudinal patterns is using tidal analysis. Any pattern can be described by this harmonic analysis. For general definitions and explanations of tidal terms, the reader is referred to Forbes (1995). In a first step, longitudinal averages are subtracted from the bin readings hour by hour. This removes the mean local time variation, as shown in Figure 4. The mean-free distribution in Figure 6b reveals already clear tidal signatures. ΔRC structures are propagating eastward towards later local time hours. Since we do not have residual values over all 24 local time hours, a self-consistent tidal analysis cannot be applied. Rather, we have to guess most probable tidal components and test by model fitting how well they represent the data. In this case, we have identified the semidiurnal symmetrical tide S0 (cf. Figure 6c) as the most suitable component for modulating ΔRC. Mathematically this can be expressed as

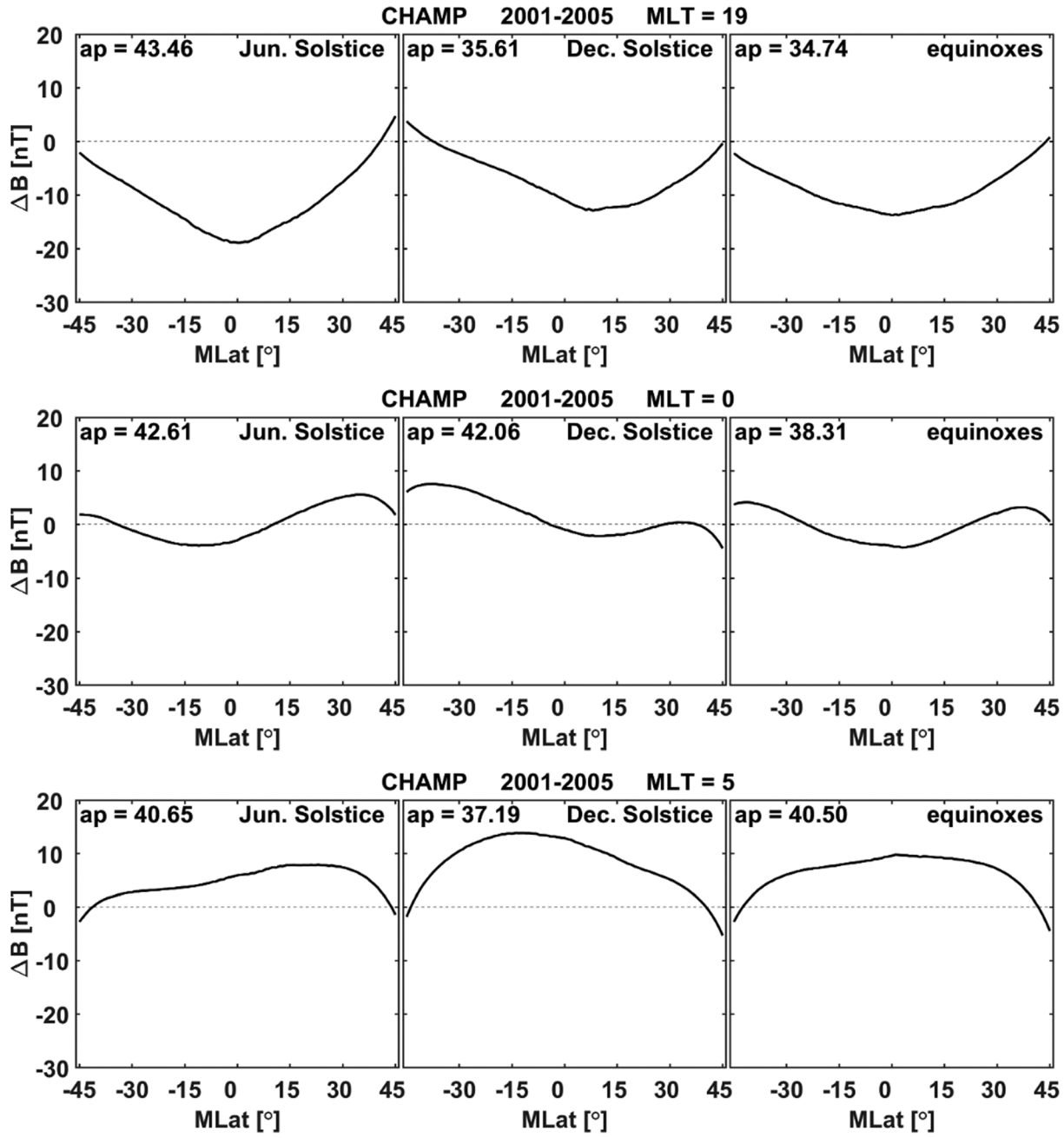

FIGURE 5. Latitude profiles of mean total field residuals for different seasons (from left to right June, December months, and combined equinoxes). Examples are presented for the local times 19, 24, and 05 MLT in the top, middle, and bottom rows, respectively.

$$\Delta RC(S0) = A\ \cos\left(\frac{\pi}{6} MLT - 2\lambda - \varphi\right), \tag{4}$$

where A is the amplitude, λ is the longitude, and φ is the phase in local time when the wave crest passes the Greenwich meridian. The obtained tidal amplitude of ΔRC amounts to 4.1 nT, and the phase is 7.11 hour. This kind of tidal component represents a UT dependence of ΔRC values. In other words, at 7:07 UT and 19:07 UT, the residuals are enhanced globally by 4.1 nT; while at 01:07 UT and 13:07 UT, the values are diminished by 4.1 nT. This tidal effect adds on top of the mean local time dependent residuals presented in section 3.1. The random distribution of the residuals (see Figure 6d) confirms our choice of tidal component.

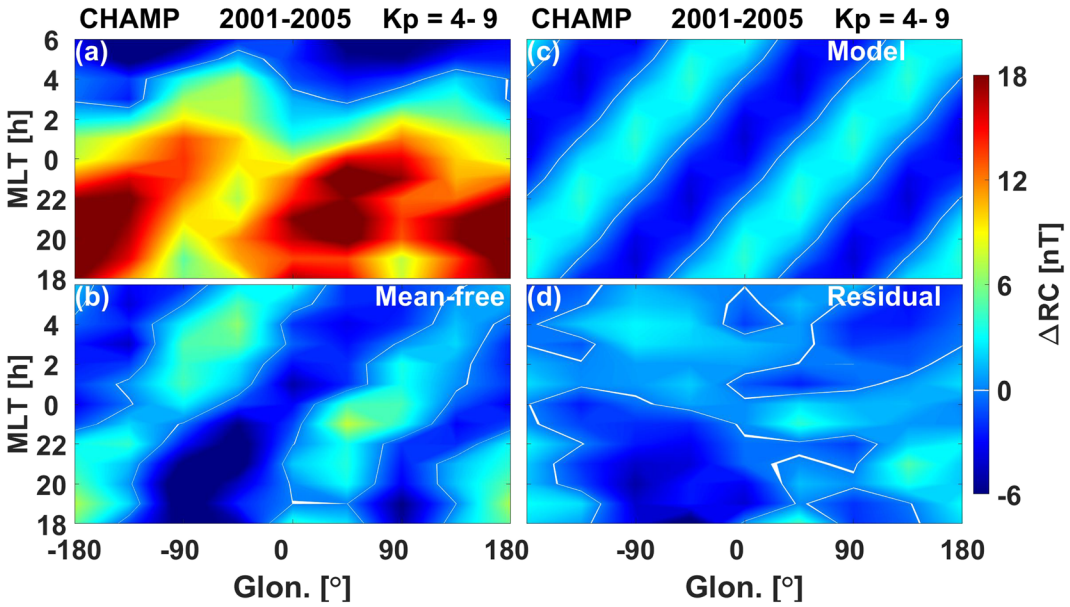

FIGURE 6. (a) Mean residual *ΔRC* distribution in a longitude versus local time frame for high magnetic activity and averaged over all seasons; (b) the mean-free distribution of *ΔRC* achieved by subtracting the longitudinal means; (c) semidiurnal tidal model fitted to the mean-free observations; (d) remaining residuals.

4. Discussion

In the previous sections, we have shown that the CHAOS-6 model represents CHAMP magnetic field observations very well for magnetically quiet conditions with Kp = 0 to 1. This is the activity range where the model is made for. But already at moderate activity levels, Kp = 2 to 3, systematic residuals, with several nT amplitude emerge, caused by magnetospheric currents. These residuals get progressively larger for increasing magnetic activity. As it is obvious from Figure 4, there is a clear local time dependence of the disturbance level. The so-called partial ring current effect is known to generate stronger negative deflections in the evening sector and reduced values in the morning sector during the magnetic storm main phase. Le et al. (2011) presented for a number of storms the local time distribution of low-latitude disturbances from C/NOFS observations. They revealed a systematic asymmetry of the ring current signal towards the 18 MLT sector, independent of the activity level. The *ΔRC* residuals derived here exhibit largest amplitudes between 20 and 21 MLT. And the switch from negative to positive residuals occurs between 03 and 04 MLT. For an activity level of Kp = 4.7, we read from Figure 4 a peak value of about 12 nT around 21 MLT. Lühr et al. (2017) investigated statistically the Kp-dependence of the D_{ST} asymmetry. They report an enhancement of the ring current effect by 17.4 nT centered at 18.1 MLT when considered events in the Kp range 4–6. The mean Kp value of that range can be assumed to be close to Kp = 4.7 when considering the typical Kp distributions. By comparing the two results, we may conclude that CHAOS-6 has not only reduced the dawn/dusk asymmetry by about 6 nT but also shifted the remaining peak by about 3 hr to later local times. These two numbers imply that the model applies on average an asymmetry correction with about half the actual amplitude that it is centered at about 15 MLT rather than 18 MLT. The symmetric part of magnetospheric currents seems to be corrected on average reasonably well.

It has to be noted that our assessment of residuals is limited to the nighttime hours when ionospheric currents are low. The simplest assumption for the dayside is a continuation of the asymmetric disturbances as pure diurnal variation.

We have shown that the CHAOS-6 residuals do not only vary with local time, but they have also a dependence on season. Clearly, more positive values are found in the winter hemispheres. It has earlier been reported (e.g., Lühr & Zhou, 2020) that the asymmetric storm-time disturbance is stronger in the winter than in the summer hemisphere. This has at least two consequences for the magnetospheric current corrections: (i) since the determination of the ring current index (D_{ST} or RC) is mainly based on observatories in the

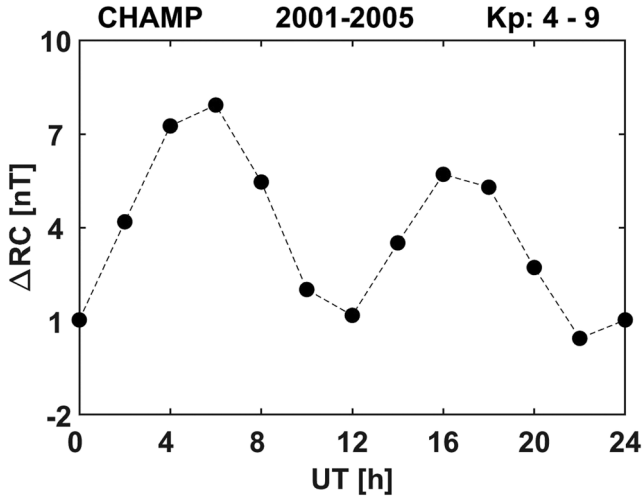

FIGURE 7. Semidiurnal Universal Time dependence of the mean residual *ΔRC* for periods of high magnetic activity. All seasons and all considered local times (nighttime) have been taken into account.

northern hemisphere, a December months bias results; (ii) a correction of the so-called ring current effect by degree 1 external SHA functions is not sufficient during most parts of the year.

Lühr and Zhou (2020) have shown that at least the asymmetric parts of the storm-time disturbances do not result from the ring current but from antisunward auroral net currents that are connected on their day and night side ends by field-aligned currents reaching out to the magnetopause on the dawn and dusk flanks where the currents are closing. Their near-Earth disturbance signals are coming primarily from the large-scale FACs. Therefore, different disturbance levels can be observed in the two hemispheres. These authors also show the dominance of antisunward auroral currents in the winter hemisphere. As a consequence, seasonal asymmetries of hemispheric disturbance distributions are expected in the residuals.

The correction of the magnetospheric current effects is parameterized in CHAOS-6 by the RC index, which is based on readings from 21 observatories. Only six of them are located in the southern hemisphere. This ratio 15 to 6 is according to Item (i) above causing a December months bias of the index. This effect does not seem to be too large. At least, there is in Figure 5 some evidence that the June residuals are systematically more negative, which may point at the underestimation of the RC index during that season. But more significant seems to be the effect of Item (ii). CHAOS-6 assumes a spatially homogeneous external magnetic field at near-Earth space, considering no hemispheric asymmetries. This is not justified during solstice seasons. Due to stronger antisunward currents flowing through the connected FACs in the winter hemisphere, in particular on the duskside, more negative deflections are generated there. This trend we observe during both solstice seasons.

A rather surprising observation is the longitude dependence of the *ΔRC* residuals. The derived wave-2 pattern, resembling a semi-diurnal S0 tide, can be interpreted as a Universal Time dependence of the residuals. For checking our inferences, we have plotted in Figure 7 the variation of the derived *ΔRC* over UT time during high-activity periods, including all seasons and all considered local times. Clear maxima appear around 06 and 17 UT. These times and the amplitude are close to the values derived by our tidal analysis in section 3.3. Different reasons could be the cause for such an Earth-fixed pattern, for example, (i) A UT-dependent deficit of the RC determination with a 12-hr period (ii) or the wobble between the SM and GSM frames. Around 06 and 18 UT currents in these frames are parallel to each other; around 12 and 24 UT largest inclination angles are reached between them. More dedicated studies are required for explaining these observations of longitude dependence.

5. Summary and Conclusions

In this study, we have investigated the residuals in total B-field resulting from the difference, observations minus the recent CHAOS-6 model. The 5 years of CHAMP high-resolution magnetic field data, 2001–2005 have been used. Investigations are limited to nighttime hours 18–06 MLT. Although CHAOS is designed as a quiet-time magnetic field model, we have tested its reliability outside its validity range. The derived mean residuals can predominately be related to magnetospheric current effects, and in particular the asymmetric parts. Our important findings can be summarized as follows:

1. The symmetric part of the ring current effect is modeled reasonably well up to magnetic activity levels of about Kp = 4. Some seasonal bias is observed due to the dominance of northern hemisphere observatories contributing to the RC index. This results in an underrepresentation of the ring current effect around June solstice.
2. With increasing magnetic activity negative total *B* residuals appear in the evening to postmidnight local time sector, while residuals are positive in the morning sector. This typical asymmetry of the storm-time disturbance is well-known for active periods. CHAOS-6 does not account properly for this asymmetry. The modeled local time-dependent amplitude seems to have on average only half the actual value, and

its peak value appears about 3 hr too early in local time. As a consequence, mean local time-dependent residuals within the range of ±12 nT appear at an activity level of Kp ~ 4.7.

3. The mean results from 5 years considered represent annual averages. However, the residuals exhibit also significant seasonal variations. The derived ΔRC differences are clearly larger in the winter than in the summer hemisphere. This implies both a global underrepresentation of the ring current effect around June solstice and an obvious latitudinal asymmetry of the disturbance signal during solstice seasons (weaker in the summer hemisphere). The applied degree 1 spherical harmonics analysis to the external field contribution is not able to correct for that hemispheric dependence, and the degree 2 terms are kept constant over the year (see Equation 1 and explanation).
4. The residual ring current effect, ΔRC, shows also a longitude dependence. This appears as a semidiurnal S0 tidal pattern. Such a tidal signal represents a UT-dependence of ΔRC with a 12 hr period. At present, it is not clear whether this is a real modulation of magnetospheric currents or an artifact introduced by the model approach.

All the presented residuals show that the CHAOS-6 model, outside its definition region (Kp = 0–2), has deficits in representing the magnetospheric current contributions properly for times of medium and enhanced magnetic activity. Main reason for it is that the actual temporal and spatial characteristics of these currents are not taken properly into account. For improving the situation, it would be desirable to determine in a statistical study the near-Earth magnetic signals of the large-scale magnetospheric currents and their dependences on magnetic activity, local time, Universal Time, season, latitude, and longitude. Based on such a climatological description, magnetospheric contributions could be parameterized much more efficiently in geomagnetic field models. Other geomagnetic field model families (e.g., GRIMM, POMME, CM) are expected to have their own limitations in magnetospheric field representation, but investigating those is beyond the scope of this study.

Acknowledgments

The authors thank Ingo Michaelis for his great effort in improving the CHAMP Level 3 magnetic field data. The CHAMP mission was sponsored by the Space Agency of the German Aerospace Center (DLR) through funds of the Federal Ministry of Economics and Technology. The CHAMP magnetic field data (product identifier: CH-ME-3-MAG) are available at ftp://magftp.gfz-potsdam.de/CHAMP/L3_DATA. Coefficients and software for running the CHAOS-6 model can be downloaded from http://www.spacecenter.dk/files/magnetic-models/CHAOS-6/. The magnetic activity indices Kp and a_p have been downloaded from the GFZ, German Research Centre for Geosciences at ftp://ftp.gfz-potsdam.de/pub/home/obs/kp-ap/. The work of Yun-Liang Zhou is supported by the National Key R&D Program of China (No. 2018YFC1407303).

References

Finlay, C. C., Olsen, N., Kotsiaros, S., Gillet, N., & Tøffner-Clausen, L. (2016). Recent geomagneticsecular variation from swarm. *Earth, Planets and Space*, *68*, 1–18.

Forbes, J. M. (1995). Tidal and planetary waves. In R. M. Johnson & T. L. Killeen (Eds.), *The upper Mesosphere and Lower Thermosphere: A Review of Experiment and Theory* (Vol. 87, pp. 67–88). Washington, DC: AGU, Geophysical Monograph.

Hapgood, M. A. (1992). Space physics coordinate transformations: A user guide. *Planetary and Space Science*, *40*(5), 711–717. https://doi.org/10.1016/0032-0633(92)90012-D

Le, G., Burke, W. J., Pfaff, R. F., Freudenreich, H., Maus, S., & Lühr, H. (2011). C/NOFS measurements of magnetic perturbations in the low-latitude ionosphere during magnetic storms. *Journal of Geophysical Research*, *116*, A12230. https://doi.org/10.1029/2011JA017026

Lesur, V., Rother, M., Wardinski, I., Schachtschneider, R., Hamoudi, M., & Chambodut, A. (2015). Parent magnetic field models for the IGRF-12GFZ-candidates. *Earth, Planets and Space*, *67*(1), 1–15.

Lesur, V., Wardinski, I., Rother, M., & Mandea, M. (2008). GRIMM: The GFZ reference internal magnetic model based on vector satellite and observatory data. *Geophysical Journal International*, *173*(2), 382–394. https://doi.org/10.1111/j.1365-246X.2008.03724.x

Lühr, H., Xiong, C., Olsen, N., & Le, G. (2017). Near-Earth magnetic field effects of large-scale magnetospheric currents. *Space Science Reviews*, *206*, 521–545. https://doi.org/10.1007/s11214-016-0267-y

Lühr, H., & Zhou, Y.-L. (2020). Relation between the asymmetric ring current effect and the anti-sunward auroral currents, as deduced from CHAMP observations. *Annales de Geophysique*, *38*, under discussion. https://doi.org/10.5194/angeo-2020-3

Maus, S., Manoj, C., Rauberg, J., Michaelis, I., & Lühr, H. (2010). NOAA/NGDC candidate models for the 11th generation international geomagnetic reference field and the concurrent release of the 6th generation Pomme magnetic model. *Earth, Planets and Space*, *62*(10), 729–735. https://doi.org/10.5047/eps.2010.07.006

Olsen, N., Lühr, H., Finlay, C. C., Sabaka, T. J., Michaelis, I., Rauberg, J., & Tøffner-Clausen, L. (2014). The CHAOS-4 geomagnetic field model. *Geophysical Journal International*, *197*(2), 815–827. https://doi.org/10.1093/gji/ggu033

Reigber, C., Lühr, H., & Schwintzer, P. (2002). CHAMP mission status. *Advances in Space Research*, *30*(2), 129–134. https://doi.org/10.1016/S0273-1177(02)00276-4

Rother, M., & Michaelis, I. (2019). CH-ME-3-MAG—CHAMP 1 Hz combined magnetic field time series (level 3). *GFZ Data Services*. https://doi.org/10.5880/GFZ.2.3.2019.004

Sabaka, T. J., Olsen, N., & Langel, R. A. (2002). A comprehensive model of the quiet-time,near-earth magnetic field: Phase 3. *Geophysical Journal International*, *151*(1), 32–68. https://doi.org/10.1046/j.1365-246X.2002.01774.x

Sabaka, T. J., Olsen, N., Tyler, R. H., & Kuvshinov, A. (2018). A comprehensive model of Earth's magnetic field determined from 4 years of swarm satellite observations. *Earth, Planets and Space*, *70*(1), 1, 130–26. https://doi.org/10.1186/s40623-018-0896-3

Stolle, C., Michaelis, I., & Rauberg, J. (2016). The role of high-resolution geomagnetic field models for investigating ionospheric currents at low Earth orbit satellites. *Earth, Planets and Space*, *68*(1), 110. https://doi.org/10.1186/s40623-016-0494-1